Cell. Mol. Life Sci. (2013) 70:743–759
DOI 10.1007/s00018-012-1168-1

Cellular and Molecular Life Sciences

RESEARCH ARTICLE

Alzheimer's disease risk factor lymphocyte-specific protein tyrosine kinase regulates long-term synaptic strengthening, spatial learning and memory

Eun-Jung Kim · Francisco J. Monje · Lin Li · Harald Höger · Daniela D. Pollak · Gert Lubec

Received: 25 April 2012 / Revised: 27 August 2012 / Accepted: 11 September 2012 / Published online: 25 September 2012

Abstract The lymphocyte-specific protein tyrosine kinase (Lck), which belongs to the Src kinase-family, is expressed in neurons of the hippocampus, a structure critical for learning and memory. Recent evidence demonstrated a significant downregulation of Lck in Alzheimer's disease. Lck has additionally been proposed to be a risk factor for Alzheimer's disease, thus suggesting the involvement of Lck in memory function. The neuronal role of Lck, however, and its involvement in learning and memory remain largely unexplored. Here, in vitro electrophysiology, confocal microscopy, and molecular, pharmacological, genetic and biochemical techniques were combined with in vivo behavioral approaches to examine the role of Lck in the mouse hippocampus. Specific pharmacological inhibition and genetic silencing indicated the involvement of Lck in the regulation of neuritic outgrowth. In the functional pre-established synaptic networks that were examined electrophysiologically, specific Lck-inhibition also selectively impaired the long-term hippocampal synaptic plasticity without affecting spontaneous excitatory synaptic transmission or short-term synaptic potentiation. The selective inhibition of Lck also significantly altered hippocampus-dependent spatial learning and memory in vivo. These data provide the basis for the functional characterization of brain Lck, describing the importance of Lck as a critical regulator of both neuronal morphology and in vivo long-term memory.

Keywords Lck kinase · Hippocampal synaptic strengthening · Learning and memory · Alzheimer's disease

Introduction

The non-receptor Src protein kinase was discovered more than 30 years ago by identifying the transforming single viral gene of the avian Rous sarcoma virus [1] and determining that this viral gene encoded a protein kinase associated with a phosphoprotein [2]. Several years later, the identification of Src homologues led to the proposal of a new family of non-receptor protein kinases: the Src kinase family. This family is characterized by the presence of a distinctive molecular structure consisting of several SH (Src homology) functional domains including a highly conserved catalytic (SH1) region flanked by a C-terminal auto-inhibitory phosphorylation motif [3–5]. The entire Src family is divided into two major subfamilies: subfamily-A (including Src, Fyn, Fgr and Yes) and subfamily-B (including Hck, Lyn, Blk and the protein Lck, which is also known as p56Lck [6]). An additional type of Src proteins, the Frk proteins, has also been described [3, 4]. Members from both the A and B subfamilies have been shown to play important roles in neuritic outgrowth and synaptic activity [7–14], but only Fyn, Src, Yes, Lyn and Lck have

E.-J. Kim and F. J. Monje equally shared authorship.

E.-J. Kim · F. J. Monje · D. D. Pollak
Department of Neurophysiology and Neuropharmacology, Center for Physiology and Pharmacology, Medical University of Vienna, Schwarzspanierstrasse 17, I, 1090 Vienna, Austria

E.-J. Kim · L. Li · G. Lubec (✉)
Department of Pediatrics, Medical University of Vienna, Währinger Gürtel 18-20, 1090 Vienna, Austria
e-mail: gert.lubec@meduniwien.ac.at

H. Höger
Core Unit of Biomedical Research, Division of Laboratory Animal Science and Genetics, Medical University of Vienna, Brauhausgasse 34, 2325 Himberg, Austria

been identified in the central nervous system [3, 5, 9, 15–18].

Recent clinical reports described significantly down-regulated levels of Lck in the hippocampus of Alzheimer's disease patients [19], suggesting an association of Lck with this memory-related disorder. Indeed, the human Lck gene has been located in the Alzheimer's disease-associated genetic linkage region 1p34-36 [20]. Lck has been further proposed to constitute a novel risk-gene for Alzheimer's disease [21]. These observations have increased the interest in Lck in clinical and basic neuroscience research [19–21] because, although Lck was identified in the brain approximately 15 years ago [22], it had previously been classically known for its role in T cell activation [23–25]. The role of Lck in memory remains mostly unexplored, and it is still unclear whether the down-regulation of Lck plays a pathogenic role in Alzheimer's disease.

Here, the role of Lck in the memory-related functions of the mouse hippocampus was studied, and Lck is proposed as a key regulator of both the morphological and electrical properties of neurons. It is reported that Lck critically modulates neuritic outgrowth and long-term memory. The inhibition of Lck selectively impairs the protein synthesis-dependent long-term forms of memory-related synaptic plasticity without affecting the protein synthesis-independent short-term forms of synaptic strengthening. Additionally, the selective in vivo inhibition of Lck significantly impairs hippocampus-dependent spatial learning and memory.

To the best of our knowledge, these data constitute the first comprehensive in vitro and in vivo functional characterization of Lck in the mammalian brain, suggesting that Lck is a critical mediator of the acquisition and long-term maintenance of memories, which are the most salient processes impaired in Alzheimer's disease. Because down-regulated levels of Lck have been reported in the hippocampus of patients with Alzheimer's disease [19], current animal studies may provide the first functional evidence linking the effects of the in vivo down-regulation of Lck with some of the memory-related deleterious structural and functional features that are also observed in the pathophysiology of Alzheimer' disease in humans.

Materials and methods

Animals and housing

Adult C57BL/6J male mice (Janvier, France) that were 10–12 weeks old were housed in pairs in standard transparent laboratory cages in a temperature-controlled colony room (21 ± 1 °C) and were provided with food and water ad libitum. The mice were maintained on a 12-h light/dark rhythm, and the cages were cleaned once a week. The experiments were performed under license of the federal ministry of education, science and culture, which includes an ethical evaluation of the project (Project: BMBWK-66.009/0036/BrGT-2006). The housing conditions and the maintenance of the animals were in compliance with European and national regulations. All efforts were exerted to minimize the degree of animal suffering and the number of animals used.

Hippocampal culture

Postnatal mouse (day 0–2) hippocampal neurons were dissociated and cultured according to standardized procedures [26] and complemented with glial support cultures as previously described [27].

Cell viability assay

To evaluate the effects on cell survival of the different compounds used in this work (damnacanthal, Herbimycin-A, and 4A6H), hippocampal neurons (DIV1) were plated on 96-well plates at an average density of 5×10^4 cells/well, and MTT assays were performed in quintuplicate for each experimental compound. The colorimetric MTT assays were conducted as previously described [28]. The cells were treated with increasing concentrations of the respective compound or DMSO alone as a control and incubated with 0.5 mg/mL MTT-formazan (Sigma-Aldrich, Poole, Dorset, UK) at 37 °C under 5 % CO_2 for 1–4 h and then washed in PBS. The blue formazan reduction product, which is produced by the action of succinate dehydrogenase in living cells, was dissolved in 100 µL of DMSO and incubated for 10 min. The optical density was then measured at 550 nm using a BioTek Ultra Microplate reader BL808 (BioTek, Winooski, VT, USA). The data are expressed as the percentage of viable cells compared with the number of control cells (100 % viability), as determined by MTT reduction.

Morphological evaluation

DIV0 cells were treated with different concentrations of Damnacanthal (Enzo Life Sciences) for 24 h as described in the text. A morphological analysis was performed using conventional confocal microscopy (Axiovert 200M; Zeiss, Vienna, Austria). The images were analyzed using the public domain open source software ImageJ (http://rsbweb.nih.gov/ij/). The degree of neuritic outgrowth was evaluated using previously described parameters [29, 30]. Briefly, low-density hippocampal neuronal cultures were established and used for the morphological analysis. Only those neurons that were growing in isolation, that is,

neurons whose branches did not make visible contacts with any other cell as determined using a ×40 objective and bright field microscopy, were used for the analyses. The field areas were visualized under the microscope, and representative pictures from the neurons obtained from the different experimental conditions were obtained. The ImageJ software was used to manually trace-track and measure the length of individual neurites for each of the different cells measured, and only primary (derived from the soma) neuritic branches were analyzed. Because no significant differences in the number of neuritic extensions derived from the soma were observed, we arbitrarily selected for analysis only those cells with neuritic branches more than 10 μm in length. The cells were imaged by a researcher blinded to the experimental conditions. Comparisons between the experiments (triplicate per group) were performed using different animals and cell batches. A solution of 1 % B27 supplement media was used during drug studies. On average, 25–35 isolated cells per group were analyzed.

Transfection

The DIV0 cells were transfected with Lipofectamine® LTX (Invitrogen, Carlsbad, CA, USA) and Nupherin™-neuron (Biomol, Plymouth Meeting, PA, USA) according to the manufacturer's protocols with minor modifications that have been previously described [31]. A genetically based approach that was previously used to successfully induce silencing of the Lck protein [32] was followed in this work using the murine Lck shRNAs and the scrambled nonspecific shRNAs controls in the pGeneClip hMGFP vector (Qiagen, Hilden, Germany). Briefly, 0.5 μg of the murine Lck shRNAs or the scrambled nonspecific shRNA control were incubated with 15 μg of Nupherin™-neuron in 150 μL of Neurobasal-A medium (Invitrogen) while 0.5 μL of Lipofectamine® LTX (Invitrogen) was mixed in 150 μL of Neurobasal-A medium. After 15 min, the two solutions were mixed and incubated for 45 min at 21 ± 1 °C. The neuronal cultures were incubated in 24-well plates in the resulting 300 μL mixture for 5 min, centrifuged in a swinging bucket centrifuge at 233*g* for 5 min and incubated for 2.5 h. The mixture was then substituted with 1 mL of culture medium, and the cells were transferred to a culture incubator in 5 % CO_2 at 37 °C. After 24 h, the cells were fixed in 4 % paraformaldehyde at 21 ± 1 °C for 30 min, and the paraformaldehyde was subsequently removed by washing with PBS. The confocal imaging was performed as previously described [33]. The neuritic outgrowth was also evaluated using ImageJ software (http://rsbweb.nih.gov/ij/). PC12 cells were cultured at a density of 5×10^5 cells on 10-cm Petri dishes coated with collagen (Sigma-Aldrich) and maintained in DMEM supplemented with 5 % fetal bovine serum, 10 % horse serum, and 1 % penicillin/streptomycin. The PC12 cells were transfected 12 h after plating using Lipofectamine® LTX (Invitrogen) according to the manufacturer's protocols. Briefly, 10 μg of the murine Lck shRNAs or the scrambled nonspecific shRNA control were incubated with 10 μL of PLUS™ reagent (Invitrogen) in 1 mL of Opti-MEM® reduced-serum media while 20 μL of Lipofectamine® LTX was diluted in 1 mL of Opti-MEM® reduced-serum media. After 10 min, the two solutions were combined and incubated for 25 min at 21 ± 1 °C, and the PC12 cells were then incubated in the resulting 2 mL mixture in 5 % CO_2 at 37 °C. The efficiently transfected cultures (60–70 %) were used for the subsequent RNA extraction and qRT-PCR analysis.

RNA isolation, cDNA synthesis and qRT-PCR

The RNA from the PC12 cells was isolated using the RNeasy Plus Micro Kit (Qiagen) according to the manufacturer's instructions. A 1-μg aliquot of the total RNA was used for cDNA synthesis using SuperScript III (Invitrogen) according to the protocol supplied.

The qRT-PCR experiment was performed using specific primers that have been previously described for Lck [34] and *β*-actin [35]: Lck forward (CCAGCTCACAATGCCAGCAG) and reverse (GCTCGGGGAGGGTTCATTC); *β*-actin forward (ATGGTGGGAATGGGTCAGAAG) and reverse (TCTCCATGTCGTCCCAGTTG). The qRT-PCR was performed on diluted cDNA samples using the StepOne Real-Time PCR system (Applied Biosystems) and the Power SYBR Green PCR Mastermix (Applied Biosystems) under universal cycling conditions (10 min denaturing step; 10 min at 95 °C; 40 cycles of 15 s at 95 °C, 60 s at 60 °C, and 15 s at 72 °C and a melting point analysis in 0.1 °C steps). The data were analyzed using the cycle threshold method and normalized relative to the *β*-actin expression control [35]. The experiments were performed in triplicate.

Single-cell electrophysiology

Primary hippocampal neurons (10–14 DIV) were used for electrophysiological measurements of the mEPSCs. The cells were untreated (control) or treated with either 200 nM or 10 μM damnacanthal (Biomol) 2 h prior to the recordings. The mEPSCs were acquired using the whole-cell configuration of the patch-clamp technique at 21 ± 1 °C and clamped at −70 mV. The bath solution contained 125 mM NaCl, 6 mM KCl, 2 mM $CaCl_2$, 1 mM $MgCl_2$, 1.25 mM NaH_2PO_4, 25 mM $NaHCO_3$, 15 mM glucose, and 10 mM Hepes, and the pH was adjusted to 7.4 with NaOH. Solutions of 0.5 μM tetrodotoxin (TTX) and 30 μM

bicuculline-methiodide were used to inhibit sodium-channel conductance and to suppress miniature inhibitory postsynaptic currents, respectively. The borosilicate-glass recording electrodes were pulled using a horizontal puller (Sutter Instruments) to obtain resistances of 5–7 MΩ when filled with a solution containing 140 mM KCl, 1.6 mM $CaCl_2$, 10 mM EGTA, 10 mM Hepes, and 2 mM Mg-ATP, adjusted to pH 7.3 with KOH. Events <5 pA and events with a slow rise time (>5 ms) were excluded from the analysis. The currents were obtained and analyzed using a NPI SEC-10L amplifier (NPI Electronic, Tamm, Germany) and Axon and Heka amplifiers, the FitMaster software package (HEKA Elektronik, Lambrecht, Germany) and a pClamp-10 (Axon Instruments, Foster City, CA, USA). All data are given as the mean ± SEM.

Brain slice preparation

The hippocampal slices were prepared and the electrophysiological measurements were recorded according to previously described procedures [36, 37] with minor modifications. In brief, male (7–11 weeks old) C57BL/6J mice (Janvier, France) were narcotized with CO_2, swiftly sacrificed by cervical dislocation and decapitated. The brains were quickly extracted and immersed in ice-cold (~4 °C) "dissection" artificial cerebrospinal fluid solution (D-ACSF) containing 125 mM choline-chloride, 2.5 mM KCl, 25 mM $NaHCO_3$, 0.5 mM $CaCl_2$, 6 mM $MgCl_2$, 25 mM D-glucose, and 1.25 mM NaH_2PO_4 (all from Sigma-Aldrich, Vienna, Austria).

The hippocampi were isolated while the tissue was submerged in D-ACSF. Transverse slices (400 µm) were obtained using a McIlwain Tissue Chopper (Mickle Laboratory Engineering, UK). The slices were quickly transferred to a nylon-mesh floating in a home-customized interface chamber containing "recording" artificial cerebrospinal fluid solution (Rec-ACSF) maintained at 21 ± 1 °C. The slices were allowed to recover for 1 h at 21 ± 1 °C and 30 min at 28 °C before the recordings were performed. During the dissection, recovery and recording, the slices were continuously bubbled with a saturating carbogen mixture (95 % O_2/5 % CO_2) adjusted to pH 7.4. The field potential recordings of the slices were performed at a temperature of 28 °C. The Rec-ACSF solution contained 125 mM NaCl, 2.5 mM KCl, 25 mM $NaHCO_3$, 2 mM $CaCl_2$, 1 mM $MgCl_2$, 25 mM D-glucose, and 1.25 mM NaH_2PO_4 (all from Sigma-Aldrich).

Slice electrophysiology and data analysis

It has been reported that, whereas a brief period of hippocampal theta-burst stimulation induces a protein synthesis-independent short-term synaptic potentiation, prolonged stimulation gives rise to a sustained or long-term protein synthesis-dependent synaptic potentiation [38–40]. Here, an electrical stimulation was applied to the hippocampal Schaffer collateral/associational commissural pathway using a home-customized bipolar tungsten electrode insulated to the tip (50 µm tip diameter). The stimuli were delivered using an ISO-STIM 01D isolator stimulator (NPI Electronics, Tamm, Germany). The field excitatory postsynaptic potentials (fEPSPs) were obtained from the CA1 stratum radiatum area of the hippocampus using borosilicate glass micropipettes that yield resistances of 2–5 MΩ when filled with Rec-ACSF. The stimuli (80 µs) were delivered at intervals of 15 s, and the slope of the decaying phase (20–80 % of the peak amplitude) of the fEPSP was used to estimate the strength of the synaptic transmission. Stable baseline measurements were obtained for at least 10 min using stimulation intensities eliciting ~40 % of the maximal inducible response (5 min before the theta-burst stimulation). The early or short synaptic potentiation (E-LTP) was induced by applying a single high-frequency train of pulses (pulses delivered at 100 Hz for 1 s, 80 µs/pulse) as previously described [38–40]. The late or long-term (L-LTP) form of synaptic potentiation was induced by four trains of theta-burst stimulation (15 bursts of four pulses at 100 Hz (80 µs/pulse) with inter-burst intervals of 200 ms and inter-train intervals of 5 min) [38–40]. The recordings (n = 10–20) were obtained for at least 30 min after each standard LTP-inducing stimulation protocol. The slope values from the fEPSPs obtained after the theta-burst stimulation were normalized to the average of their respective baseline slopes. The data were obtained using an AxoClamp-2B amplifier (Bridge mode) and a Digidata-1440 interface (Axon Instruments), and the pClamp-10 Program software (CA/Molecular Devices, USA) was used for the data analysis.

Behavioral analysis

Two groups of animals (10 per experimental group; one group of untreated controls, which were injected with a saline/DMSO solution, and a second group injected with damnacanthal/DMSO) were used for the behavioral analysis (an extra set of different animals was used for the western blot analysis; see below). For the behavioral studies, damnacanthal (5 mg/kg) or saline with DMSO (final concentration of 8 %) was injected i.p. at an injection volume of 10 mL/kg. All the experimental trials in which the behavior was examined throughout the entire period of study were preceded by the corresponding i.p. injection. The behavioral analyses were performed 45 min after the injection.

Basic neurological examination

To examine the effects of the Lck inhibitor damnacanthal on the major neurological behavioral features and reflexes of the experimental subjects, a series of tests were implemented 45 min after injection as previously described [33, 41].

Open field (OF)

The open field consisted of a rectangular box of Plexiglas (40 × 40 × 60 cm) in which locomotor activity was monitored for 1 h using a CCD camera (Panasonic, Secaucus, NJ, USA). The locomotor activity, which was evaluated 45 min after the i.p. injection as the total distance traveled (cm), was automatically measured using a Limelight video tracking system (Limelight Actimetrics, Elmwood, IL, USA). A solution of 70 % ethanol was used to clean the equipment between each examination.

Rota rod

The motor coordination and balance were tested using an automated 5-station mouse system (Model ENV-575MA; Med-Associates, Georgia, Vt, USA). The animals were tested 45 min after the i.p. injections using a previously described protocol [42] with minor modifications. The mice were placed on the rod when the rod started moving, with the snout of the animal facing the same direction as the moving belt, and the speed of rotation was set to systematically increase from 4 to 40 rpm over a 5-min period. The time until the mouse fell off the drum (latency) was recorded and used for the analysis.

Morris water maze

The Morris water maze (MWM) consisted of a standard circular pool (122 cm diameter with walls 76 cm deep). The mice were trained to escape by swimming to a hidden platform located 1.5 cm beneath the water surface. The platform location was identified using distal extra-maze cues attached to the room walls and remained constant during the entire experiment. The pool (with a water temperature of 21 ± 1 °C) was monitored using a digital camera, and the pool image was digitally divided into four quadrants by a computerized tracking/image analyzing system (Limelight Actimetrics). From a total of 20 mice, 10 mice were used per group (control vs. treated). Each group was subdivided into two sub-groups of 5 mice each. The hidden platform was changed from south-east to north-east between sub-groups. The platform was placed in the middle of the respective quadrant and remained at the same position during the acquisition phase (see below). Each day, and 45 min before the first training trial, the mice were injected either with damnacanthal or with a diluting saline control solution. The day before starting the measurements, each mouse received a pre-acquisition session in which it was placed directly on the platform and required to stay for a minimum of 15 s. The mice were then allowed to have 30 s of a free swimming period before being guided back to the platform. This pre-acquisition consisted of 3–4 test trials in which each mouse was required to climb by itself onto the platform. On the first day of the measurements, the mice received single and final reinforcement trials in which the mice were placed directly onto the hidden platform and required to remain for at least 15 s. The acquisition phase then began and consisted of three trials per day (with inter-trial intervals of 15 min) in which the mice were placed into the pool containing the hidden platform and allowed to swim freely. The behavioral measurements for each acquisition trial started when the mouse was released into the water, and the recordings were obtained for at least 90 s. The mice were released while facing the outer edge of the pool at one of the quadrants (except the quadrant in which the platform was located). A trial was terminated when the animal located the platform and remained on it for at least 15 s. During the acquisition, the mice lined up and were tested successively in trains of five. Mice that failed to locate the platform within the first 90 s of the acquisition phase were manually placed onto the platform and required to remain for 15 s. The acquisition phase was extended for a period of 3 days. After the acquisition phase, the mice underwent a 1-day probe trial in which the platform was removed. In this trial, the mice were released from the longest distance to the platform and were allowed to swim freely for 60 s. Measurements of the swimming path taken by the mouse were recorded, and the proportion of swimming time and/or the path length spent in each quadrant of the pool was analyzed.

Western blotting

The dose–response was examined to evaluate the inhibitory effects and specificity of damnacanthal in vivo. Thus, two individual mice per group, which were not involved in the behavioral analysis, were subjected to intra-peritoneal injections with 2.5, 5, or 10 mg/kg of damnacanthal according to the same administration procedures used for the animals subject to the behavioral experiments. The animals were narcotized with CO_2 45 min after injections, rapidly underwent cervical dislocation and were immediately decapitated. The hippocampi were then quickly dissected and snap-frozen in liquid nitrogen, and the tissue was stored at −80 °C until used. The hippocampal tissue was ground under liquid nitrogen and homogenized in a protein lysis buffer containing 10 mM Tris–HCl (pH 7.5),

Fig. 1 Selective inhibition of Lck impairs neuritic outgrowth. (**A**) *a* An MTT assay was used to evaluate the cytotoxicity of different concentrations of damnacanthal. None of the displayed concentrations induced high levels of cell mortality. *b*, *c* Treatment with the Lck-specific inhibitor damnacanthal (200 nM) did not induce changes in the length of neurites (two-tailed $P > 0.05$) compared with those of untreated control hippocampal cells. (**B**) *a* Representative cells obtained from a group of untreated primary cultured control hippocampal neurons presented a marked development of neuritic processes (*a left*, *b*), whereas the specific inhibition of Lck with 10 μM damnacanthal resulted in a marked reduction (two-tailed $P < 0.0001$) in the development of neuritic processes (*a right*, *b*). In (*b*, *c*), the representative images of the results of western blot assays indicate that 10 μM damnacanthal is more efficient than 200 nM damnacanthal in hampering the levels of 394-phospho-Lck in primary cultured mouse hippocampal neurons. (**C**) Effect of shRNA-based inhibition of Lck on neuritic outgrowth. *a* Representative neuron transfected with the green fluorescent protein (GFP) alone. *b* Representative neuron transfected with a scrambled-control version of the Lck shRNA gene-silencing sequence (scrambled-control shRNA). *c* Representative neuron transfected with a specific and previously characterized Lck shRNA gene-silencing sequence (LCK#1). *d* Histograms representing the changes in the average neuritic length in response to neuronal transfection with four specific and previously characterized Lck shRNA gene-silencing sequences (LCK#1–4), all of which resulted in a pronounced reduction of neuritic outgrowth compared with the neurons transfected with the green fluorescent protein (GFP) alone (*a*) or with cells transfected with the scrambled-control version of the Lck shRNA gene-silencing sequence (*b*). *d* Average of neurite length/cell: ANOVA *P* value is <0.0001; Tukey–Kramer post hoc tests; GFP versus scrambled-control shRNA ns $P > 0.05$; GFP versus LCK#1 *** $P < 0.001$; GFP versus LCK#2 *** $P < 0.001$; GFP versus LCK#3 *** $P < 0.001$; GFP versus LCK#4 *** $P < 0.001$; scrambled-control shRNA versus LCK#1 *** $P < 0.001$; scrambled-control shRNA versus LCK#2 *** $P < 0.001$; scrambled-control shRNA versus LCK#3 ** $P < 0.01$; scrambled-control shRNA versus LCK#4 *** $P < 0.001$; LCK#1 versus LCK#2 ns $P > 0.05$; LCK#1 versus LCK#3 ns $P > 0.05$; LCK#1 versus LCK#4 ns $P > 0.05$; LCK#2 versus LCK#3 ns $P > 0.05$; LCK#2 versus LCK#4 ns $P > 0.05$; LCK#3 versus LCK#4 ns $P > 0.05$. (**D**) A western blot analysis (triplicate) demonstrated the presence of Lck in the PC12 cells (*a*). In *b*, the previously characterized Lck-shRNA [32] was used to inhibit Lck activity in hippocampal neurons and has the ability to hamper the levels of Lck mRNA, as demonstrated by proof-of-principle experiments in which PC12 cells were transfected with Lck-specific shRNA or scrambled-control shRNA. The mean of three experiments is indicated as a percentage of mRNA expression of the negative control (scrambled-control shRNA), as determined using qRT-PCR. (**E**) Effect of the non-receptor tyrosine kinase inhibitor Herbimycin-A on hippocampal cultured neurons neuritic outgrowth. *a* Effect of different concentrations of Herbimycin-A on the survival of neurons, as measured using the MTT assay. *b* Effect of different concentrations of Herbimycin-A on neuritic outgrowth. A one-way ANOVA and the Scheffe post-test indicated highly significant differences for 100 and 500 nM does with respect to the untreated control cells ($P < 0.001$). *c* The representative cultured hippocampal neurons treated with either 100 or 500 nM Herbimycin-A exhibited a pronounced reduction in neuritic length compared with the untreated control cells. (**F**) Effect of the selective Lck inhibitor 4A6H on the neuritic outgrowth of hippocampal cultured neurons. *a* Effect of different concentrations of 4A6H on the survival of neurons, as measured using the MTT assay. *b* Effect of different concentrations of 4A6H on neuritic outgrowth. A one-way ANOVA and the Bonferroni post-test indicated highly significant differences for 500 nM and 1 μM does with respect to the untreated control cells ($P < 0.001$). *c* The representative cultured hippocampal neurons treated with 50 nM, 500 nM or 1 μM 4A6H exhibited a pronounced reduction in neuritic length compared with the untreated control cells. To evaluate the effects on cell survival of damnacanthal, Herbimycin-A and 4A6H, hippocampal neurons (DIV1) were plated on 96-well plates at an average density of 5×10^4 cells/well, and MTT assays were performed in quintuplicate ("Materials and methods")

150 mM NaCl, 0.05 % SDS, 0.5 % Triton X100, 1 mM PMSF and a protease inhibitor cocktail (1×; Roche Diagnostics, Mannheim, Germany). Western blotting was performed essentially as previously described [43]. The membranes were blocked by incubating them with 5 % non-fat dry milk in 100 mM Tris (pH 7.5), 150 mM NaCl and 0.1 % Tween 20 (TTBS). The membranes were then incubated overnight at 4 °C with primary antibodies [Phospho Lck (Tyr 394) (1:100), Phospho Lck (Y505) (1:100); Santa Cruz Biotechnology, Santa Cruz, CA, USA; Total Lck (1:500), Phospho Fyn (1:500), Total Fyn (1:500), Phospho Fyn (1:500), Total Src (1:1,100); Abcam, Cambridge, UK]. The membranes were rinsed three times with TTBS and incubated for 1 h at 21 ± 1 °C with horseradish peroxidase-conjugated goat-anti-rabbit IgG (1:3,000) and horse-anti-mouse IgG (1:3,000) (Cell Signaling Technology, Danvers, MA, USA). The immunoreactivity was visualized using enhanced chemiluminescence (ECL; Amersham Biosciences, Piscataway, NJ, USA). Quantification was performed by chemiluminescent imaging using a FluorChem HD2 (Alpha Innotech, San Leandro, CA, USA) and the corresponding software.

Statistical analysis

To compare the two groups, two-tailed Student's *t* tests and Fisher's exact test were performed, and to compare more than two groups, a one-way ANOVA was used when appropriate. The LTP data and the latencies in the MWM were analyzed by repeated measures ANOVAs, with time points or training days, respectively, as the repeated measure (within-subject factor) and the pharmacological treatment as the between-subject factor. Significant main effects or interactions were evaluated using Scheffe's post hoc test. An α-level of 0.05 was adopted in all instances. All analyses were performed using BioStat 2009 professional software (AnalystSoft, Alexandria, VA, USA).

Results

Lck is required for neuritic outgrowth

Some Src family members have been implicated in the regulation of neuronal outgrowth [44], and the protein Lck

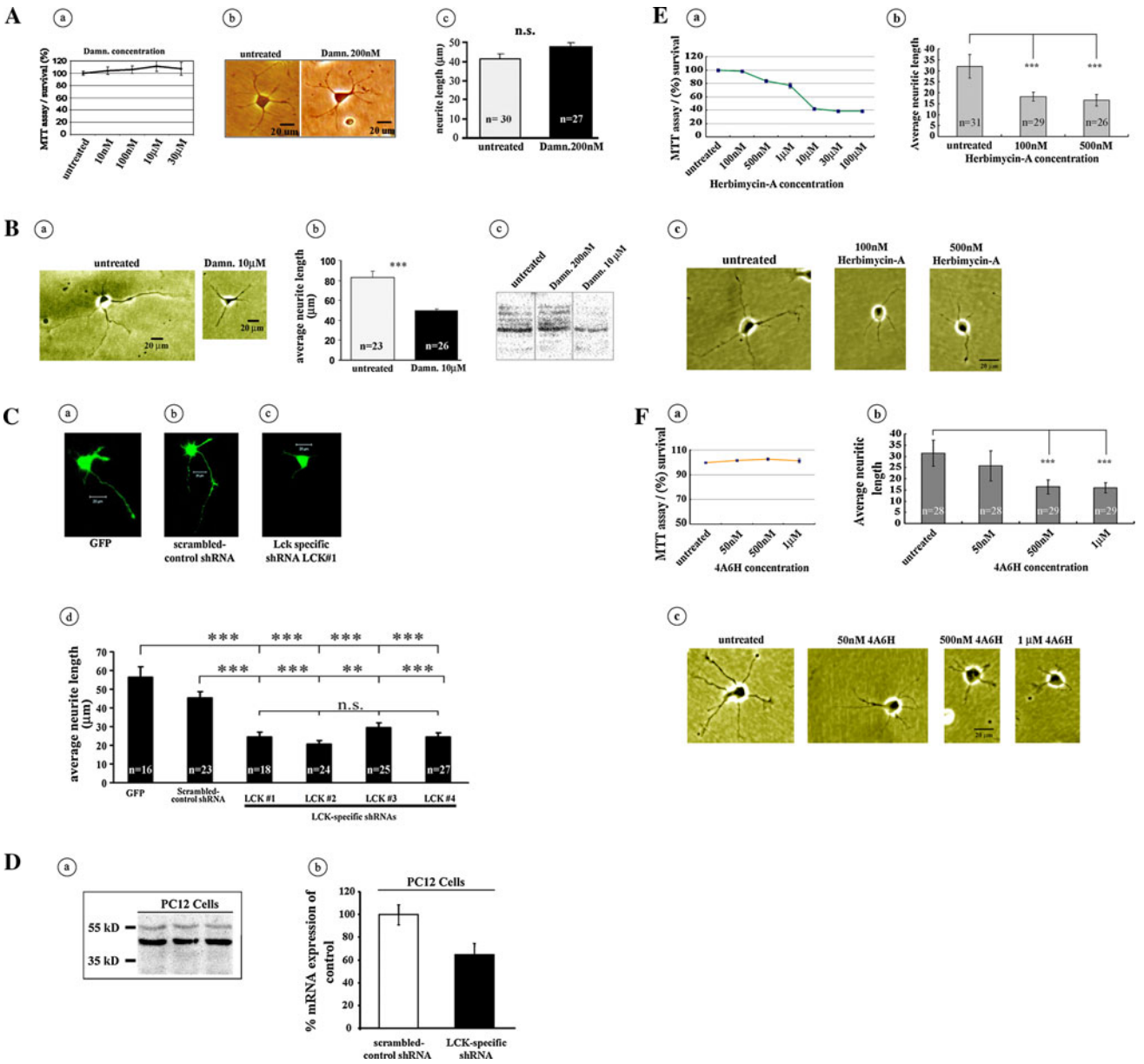

modulates differentiation in non-neuronal cells [45]. However, the involvement of Lck in the regulation of neuritic outgrowth in hippocampal neurons has remained unexplored. Using a combination of pharmacological and genetic down-regulation approaches, we examined the involvement of Lck in the modulation of neuritic outgrowth, a process central for synaptic strengthening [46, 47]. To inhibit Lck pharmacologically, we used damnacanthal, a specific inhibitor of Lck [48, 49] that has previously been used for selective Lck-inhibition in a wide range of non-neuronal cell types [50–53]. In previous reports, the inhibition of Lck with damnacanthal has been achieved using concentration ranges of 100–1,000 nM [52], 0.5–30 µM [54], 60 µM [51], or even 34 mM [53]. However, to the best of our knowledge, there are no reports addressing the specific concentrations of damnacanthal required to induce the inhibition of Lck in hippocampal neurons. Therefore, we first determined the potential neuronal toxicity of damnacanthal on cultured hippocampal neurons using a standard colorimetric MTT assay and observed that concentrations between 10 nM and 30 µM were nearly innocuous in terms of hippocampal neuron survival (Fig. 1A, a).

We next treated primary cultured hippocampal neurons with 200 nM damnacanthal and examined the effects on neuritic outgrowth. No differences in neuritic length were apparent between neurons treated with 200 nM damnacanthal and the corresponding internal untreated control

cells (Fig. 1A, b–c). We then tested the effects of 10 μM damnacanthal on neuritic outgrowth. In agreement with previous reports describing the involvement of other Src family members in the regulation of neuronal growth [44], 10 μM damnacanthal significantly reduced the length of neuritic processes (Fig. 1B, a–b). No significant differences in the number of neurites per cell during the different damnacanthal treatments (data not shown) were observed.

Western blot analysis using equal amounts of protein extracts and specific phospho-Lck antibodies was also used to examine the effects of 200 nM and 10 μM damnacanthal on 394-phospho-Lck-inhibition. A reduction in the levels of 394-phospho-Lck was noticeable only in the cells treated with 10 μM damnacanthal (Fig. 1B, c). We also verified the requirement of Lck for the proper development of neuritic extensions of hippocampal neurons by transfecting the neurons with Lck-shRNA-specific vectors that had previously been used for the selective silencing of Lck [32]. In agreement with the pharmacological experiments, genetic hampering of the cellular function of Lck using several different Lck-shRNA-specific silencing vectors resulted in a significant reduction in the length of neuritic extensions (Fig. C, a–d) compared with those of cells transfected with scrambled nonspecific control shRNA. To further evaluate the general biological capability of the specific Lck shRNAs as a selective inhibitor of Lck, we performed proof-of-principle Lck-shRNA transfection experiments using PC12 cells, a widely known mammalian cell line with neuronal-like morphological and functional properties. We first examined the presence of Lck in the PC12 cells using a western blot assay with a specific Lck antibody and detected a band of the size expected for the Lck protein (Fig. D, a). We then determined the levels of Lck in PC12 cells that had been transfected with the Lck-shRNA-specific silencing vectors and compared these levels with those from the PC12 cells that were transfected with scrambled-control shRNA using qRT-PCR. The PC12 cells that were transfected with the Lck-shRNA-specific silencing vectors exhibited reduced levels of Lck (Fig. 1D, b).

These two independent pharmacological and genetic experiments indicate that, although Lck does not appear to be involved in the genesis of neuritic processes, it might be implicated in the subsequent developmental stages associated with the regulation of neuritic elongation, a protracted process of neuronal maturation that eventually results in the development of functional structures required for the establishment of synaptic interactions.

The agreement between the effects of the Lck-shRNA-specific silencing vectors and those of damnacanthal, together with the data from previous reports [48–54], further endorsed the use of damnacanthal as a viable experimental strategy for the selective inhibition of Lck activity. Other experiments described below provide additional support for the use of damnacanthal as a selective inhibitor of Lck.

To complement our experiments using damnacanthal, we further examined the effects on neurite outgrowth of 4A6H, which is another previously described Lck inhibitor [55]. We also examined the effects of the general non-receptor tyrosine kinase inhibitor Herbimycin-A, a Src-family selective tyrosine kinase inhibitor [6], as a positive-control. We first performed positive-control experiments using Herbimycin-A to test the involvement of Src-family kinases in neuritic outgrowth using primary dissociated hippocampal neurons under our experimental conditions. Because elevated concentrations of Herbimycin-A have been previously described to cause cell death [56], we first performed an Herbimycin-A dose–response assay and examined the survival of the primary dissociated hippocampal neurons (Fig. 1E, a) using the MTT assay ("Materials and methods"). For this assay, cells were treated 12 h after plating with Herbimycin-A (100 nM, 500 nM, 1 μM, 10 μM, 30 μM, and 100 μM) or 1 % DMSO as an untreated control group ("Materials and methods"). After 24 h, the cells were incubated with 0.1 mg/mL MTT-Formazan at 37 °C under 5 % CO_2 for 4 h ("Materials and methods"). We observed that concentrations of Herbimycin higher than 10 μM resulted in the death of more than 58 % of the cells, whereas Herbimycin-A concentrations of 100 and 500 nM resulted in a cell survival of more than 98 and 80 %, respectively (Fig. 1E, a). We next examined the effect of Herbimycin-A on neuritic outgrowth in hippocampal neurons using Herbimycin-A concentrations of 100 and 500 nM. Consistent with previous observations [57, 58], the inhibition of Src proteins resulted in marked alterations in the neuritic outgrowth (Fig. 1E, b–c).

We then evaluated the effects of 4A6H on cell survival. For this assay, the cells were treated 12 h after plating with 4A6H (50 nM, 500 nM, and 1 μM) or 1 % DMSO as untreated controls ("Materials and methods"). Neither of the tested concentrations of 4A6H exhibited significant cytotoxicity (Fig. 1F, a), and only 4A6H concentrations of 500 nM and 1 μM induced a reduction in the neuritic length by approximately 50 % (Fig. 1F, b–c), thus confirming the involvement of Lck in the regulation of the morphological properties of hippocampal neurons.

Lck does not mediate spontaneous excitatory synaptic transmission

We next examined the effects of the selective Lck-inhibitor damnacanthal on the electrophysiological properties of primary-cultured hippocampal neurons by measuring the miniature excitatory postsynaptic currents (mEPSCs). For

these measurements, we used matured neurons that had reached a sufficient age for the establishment of detectable, robust functional connections (10–14 DIV). Spontaneous excitatory mEPSCs were then recorded from damnacanthal-treated and untreated-control neurons. Treatment with either 200 nM or 10 μM damnacanthal did not affect the frequency or the amplitude of the mEPSCs (Fig. 2A, B; two-tailed P values > 0.05), suggesting that Lck does not play a major role in the regulation of presynaptic excitatory neurotransmitter release and basal synaptic transmission.

Inhibition of Lck impairs memory-related long-term hippocampal potentiation

We next explored the functional involvement of Lck in the regulation of NMDAR-dependent long-term synaptic plasticity. Using protocols that have been previously described [37], the fEPSP were obtained in the CA1 dendritic layer of mouse hippocampal slices before and after the application of stimulation protocols that induce either short- or long-term forms of synaptic potentiation ("Materials and methods"). The stimulations were delivered at the Schaffer collateral CA3-CA1 pathway, and recordings were obtained from untreated control slices and from slices exposed to the selective Lck inhibitor damnacanthal ("Materials and methods"). We first measured the so-called paired-pulse facilitation [59–63], a short-term form of synaptic strengthening manifested as an increase in the amplitude of an elicited excitatory post-synaptic potential evoked by a succeeding presynaptic stimulation delivered shortly after an initial conditioning presynaptic stimulation. This form of neuronal facilitation is thought to depend exclusively on the neuronal presynaptic function [59–63]. We did not observe any alterations in the synaptic facilitation induced by a conventional paired-pulse electrical stimulation protocol in any of the different groups of slices treated with damnacanthal (Fig. 3A). This result suggests that Lck might not be primarily involved in the modulation of the presynaptic events associated with the rapid changes underlying hippocampal excitatory synaptic transmission [59–63].

Standardized stimulation protocols during in vitro electrophysiological studies on mouse hippocampal slices can be implemented to functionally distinguish and separately examine both short- and long-term forms of synaptic strengthening [38–40]. Therefore, we next studied the possible involvement of Lck in both of these electrophysiologically distinguishable forms (short-term and long-term) of memory-related synaptic potentiation ("Materials and methods") using the selective Lck inhibitor damnacanthal.

We observed that the treatment of the hippocampal slices with damnacanthal did not impair either the protein

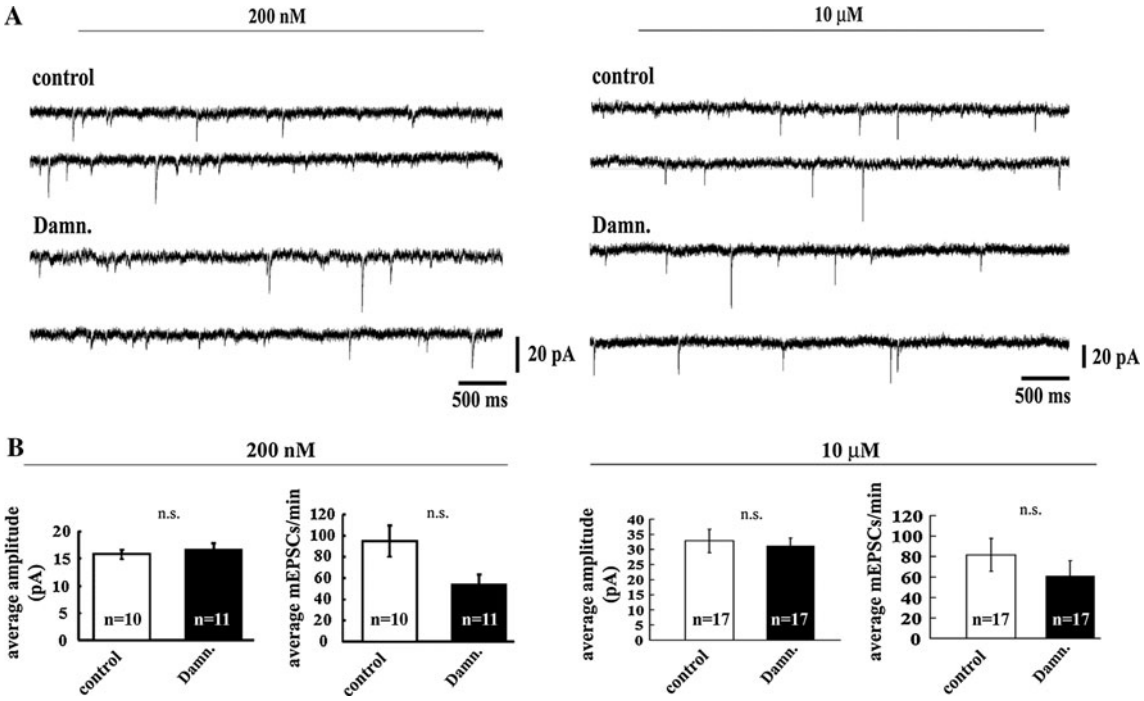

Fig. 2 Inhibition of Lck with the specific pharmacological inhibitor damnacanthal does not affect AMPA-mediated synaptic properties. **A** Representative mEPSCs traces obtained from untreated primary-cultured hippocampal neurons (control) or from neurons exposed to two different concentrations (200 nM and 10 μM) of the selective Lck inhibitor damnacanthal (*Damn.*). **B** Compared with the untreated control neurons, the inhibition of Lck did not induce statistically significant changes in either the amplitude or the frequency of the mEPSCs obtained from neurons treated with either 200 nM or 10 μM damnacanthal (*Damn.*)

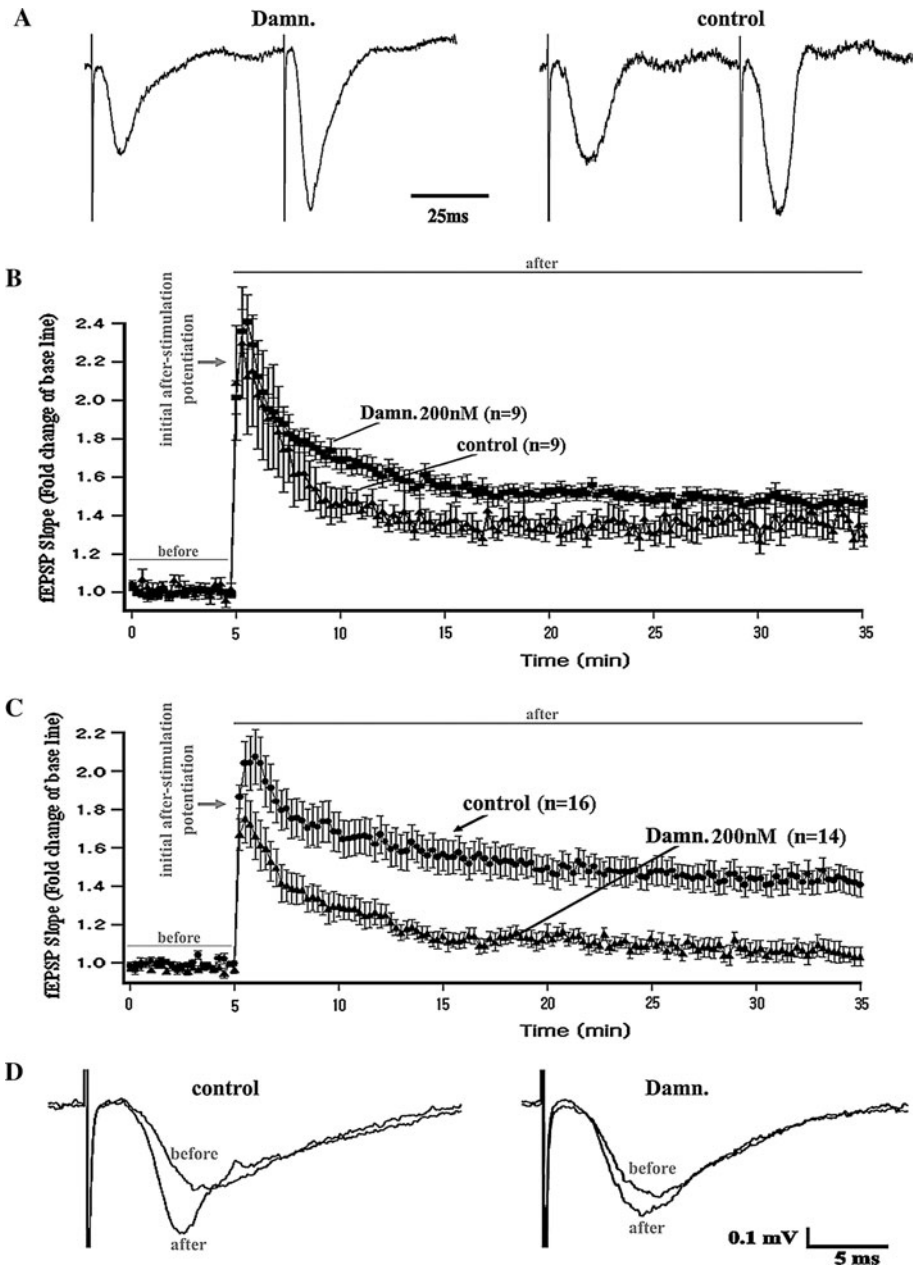

Fig. 3 Lck-inhibition and synaptic function in the CA3-CA1-Schaffer collateral pathway of hippocampal slices. **A** Representative field-potential traces (normalized to their maximal decay peak values) obtained from the control and Lck-inhibition groups of slices that underwent a paired-pulse-induced synaptic facilitation protocol (two consecutive stimulations are presented in less than 100 ms, see *Time scale bar*). The recordings indicated that the inhibition of Lck does not prevent paired-pulse-induced synaptic facilitation (*left*) but results in field potentials reflecting a synaptic activity comparable to that observed in the untreated control slices (*right*). **B** Temporal course of the fEPSP slopes obtained before (*before*) and after (*after*) the application of a brief theta-burst stimulation protocol (see "Materials and methods") that is known to only induce a protein synthesis-independent short-term form of synaptic potentiation [38–40]. The data indicate that the selective inhibition of Lck by damnacanthal (*Damn.*) did not affect this form of short-term potentiation (also known as Early-LTP). **C** Temporal course of the fEPSP slopes obtained before (*before*) and after (*after*) the application of a prolonged theta-burst stimulation protocol (see "Materials and methods") that is known to induce a long-term form of synaptic potentiation [38–40] and that requires gene transcription and the formation of newly synthesized proteins. The data indicate that the selective inhibition of Lck by damnacanthal (*Damn.*) selectively impairs this long-lasting form of synaptic potentiation (also known as Late-LTP). **D** Representative traces of the field potential recordings obtained during baseline measurements (*before*) and 30 min after the application of the L-LTP-inducing theta-burst stimulation protocol (*after*). The traces were obtained either from a group of untreated control slices (control, *left*) or from slices that underwent selective pharmacological inhibition of Lck using damnacanthal (*Damn.*, *right*; see "Materials and methods")

synthesis-independent short-term form of synaptic strengthening or its concomitant theta-burst-induced post-tetanic potentiation [Fig. 3B; repeated measures ANOVA: main effect of treatment $P > 0.05$ (n.s.); repeat (time course of LTP): $P < 0.0001$; interaction: $P > 0.05$ (n.s.)].

Conversely, in response to a completely different electrophysiological stimulation protocol pattern [38–40], Lck-inhibition resulted in a significant reduction in gene transcription and protein synthesis-dependent long-term synaptic potentiation. This effect was evaluated as the percentage of fold-change in the slope of the field potentials after application of the theta burst-induced L-LTP ("Materials and methods") compared with the low-frequency-induced baseline field responses [Fig. 3C, D; repeated measures ANOVA: main effect of treatment $P < 0.001$; repeat (time course of LTP): $P < 0.0001$; interaction: $P < 0.05$)].

As observed previously, Lck-inhibition did not prevent the generation of the initial after-stimulation potentiation during the induction of the L-LTP (Fig. 3C, D). These data suggested that Lck might play a critical role in the in vivo

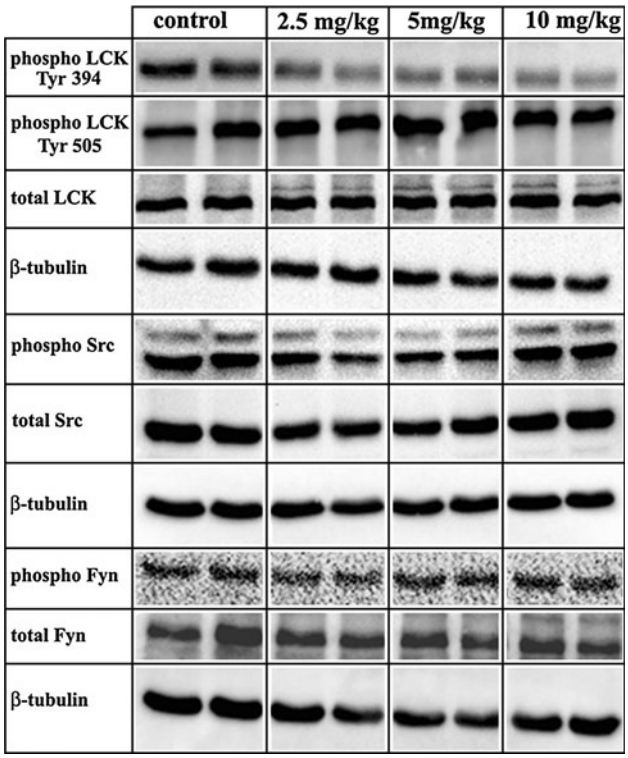

Fig. 4 Damnacanthal acts primarily as a selective inhibitor of Lck in vivo. Increasing concentrations of damnacanthal selectively inhibited the levels of the catalytically active form of the Lck protein (phospho Lck Tyr 394) in the mouse hippocampus, as determined using western blot experiments with samples of hippocampal tissue obtained from either saline control mice or damnacanthal-treated mice. Samples from one animal (two hippocampi) were used in each lane

Table 1 Primary behavioral observation screen in damnacanthal-treated and saline control mice

Type	Saline	Damnacanthal
Muscle/lower motor neuron and spinocerebellar function		
Body position	5.6 ± 0.5	5.8 ± 0.4
Atactic gait	0	0
Hypotonic gait	0	0
Impaired gait	0	0
Limb rotation	0	0
Spatial locomotion	1.9 ± 0.3	1.9 ± 0.3
Locomotor activity	4.1 ± 0.3	4.0 ± 0.0
Wire maneuver	0.5 ± 0.5	0.7 ± 0.5
Pelvic elevation	3.2 ± 0.9	2.1 ± 0.3
Tail elevation	2.7 ± 0.7	2.1 ± 0.3
Visual placing	3.7 ± 0.7	4.0 ± 0.0
Abdominal tone	4.0 ± 0.0	4.0 ± 0.0
Limb tone	4.2 ± 0.6	4.0 ± 0.5
Grip strength	4.6 ± 0.7	3.9 ± 0.6
Vestibular drop	1.0 ± 0.0	1.0 ± 0.0
Proprioception	1.0 ± 0.0	1.0 ± 0.0
Sensory function		
Transfer arousal	4.4 ± 0.7	3.8 ± 0.6
Pinna reflex	1.9 ± 0.3	2.0 ± 0.0
Corneal reflex	2.5 ± 0.5	2.2 ± 0.4
Tail pinch	1.7 ± 0.9	2.0 ± 0.0
Toe pinch	1.6 ± 0.5	1.7 ± 0.8
Finger approach	2.3 ± 0.7	2.5 ± 0.7
Finger withdrawal	3.0 ± 0.7	2.6 ± 0.8
Neuropsychiatric function		
Bizarre behaviour	0	0
Tremor/twitches	0	0
Provoked biting	2.1 ± 0.3	2.3 ± 0.7
Provoked freezing	0	0
Biting tendency	1.0 ± 0.0	1.4 ± 0.5
Autonomous function		
Palpebral closure	0	0
Skin color	4.3 ± 0.5	4.0 ± 0.0
Respiratory rate	4.0 ± 0.0	4.1 ± 0.3
Hypothermia	0	0
Urination/defecation	0.25 ± 0.4	0.2 ± 0.3
Salivation	0	0
Piloerection	1.0 ± 0.0	1.0 ± 0.0

Results of the battery of tests applied [82] to evaluate possible defects in gait or posture, changes in muscle tone, grip strength, visual acuity, temperature and other vitally important reflexes scored in control and Lck-inhibited mice groups. Throughout the manipulations, occurrence of unusual behavior, fear, irritability, aggression, excitability, salivation, lacrimation, urination and defecation were also examined in both experimental conditions. Scoring (mean ± standard deviation) was conducted following previously described parameters [82]. Higher score presents more (better, higher) activity (performance, response) or parameters are scored as present (1) or absent (0)

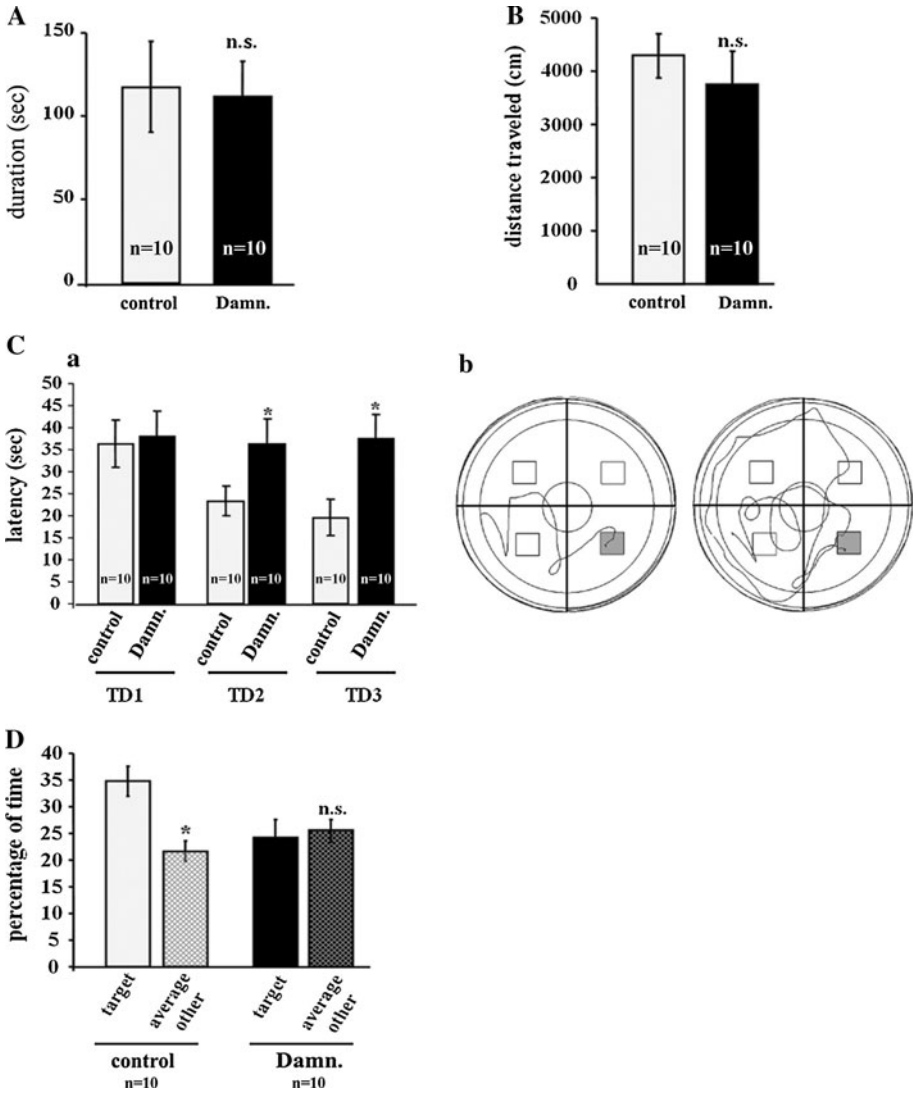

Fig. 5 The selective inhibition of Lck impairs hippocampus-dependent spatial learning and memory. For a behavioral analysis, 10 animals per experimental group (control vs. damnacanthal) were used. The control mice were injected with a saline/DMSO solution (at a final concentration of 8 % DMSO). The damnacanthal (*Damn.*)-treated mice were injected with damnacanthal/DMSO at a concentration of 5 mg/kg ("Materials and methods"). No differences in motor coordination and balance, as evaluated by the latency on the Rota rod (**A**), or in locomotor and exploratory activities (total distance traveled) in the open field (**B**) were observed in the damnacanthal-treated mice. (**C**) *a* The latency to reach the hidden platform in the Morris Water Maze during 3 days of training (TD1-3) is displayed as the average of three trials per day. The escape latency was significantly longer in the damnacanthal-treated mice compared with that of the saline controls on TD2 and TD3 ($P < 0.05$). *b* Representative swimming path traces of the saline control (*left*) or damnacanthal-treated mice (*right*) during the third training trial (TD3). (**D**) The percentage of time spent in the target quadrant (original platform location during training) versus the time spent in the remaining quadrants during the probe trial in the damnacanthal-treated and saline control mice. The data are displayed as the mean ± SEM. *n.s.* not significant; $^*P < 0.05$

regulation of long-term forms of hippocampus-dependent memory formation and maintenance.

Inhibition of Lck impairs hippocampus-dependent spatial learning and memory

We next examined the effect of the pharmacological inhibition of Lck on the acquisition and maintenance of hippocampus-dependent spatial learning and memory using the Morris Water Maze ("Materials and methods"). To examine the effect and specificity of damnacanthal in vivo, a dose–response test was first performed by injecting mice (i.p.) with 2.5, 5, or 10 mg/kg of damnacanthal. Subsequently, the levels of the total and phosphorylated forms of Lck and related Src kinases (Src and Fyn) were determined by western blotting using hippocampal protein extracts from damnacanthal-treated and control subjects. The damnacanthal treatment had no effect on the levels of total

Src, Fyn or Lck, and no changes were observed for the 505-phosphorylated form of Lck at any concentration used; however, very slight effects on the levels of the phosphorylated forms of Src and Fyn were observed (Fig. 4). In contrast, a substantial reduction in the levels of Lck that were phosphorylated at residue 394, which constitutes the active form of the protein, was observed in the hippocampal tissue of damnacanthal-treated mice at all three different concentrations used (Fig. 4). Based on the selective and pronounced inhibition of damnacanthal on the phospho-Lck-394, we decided to use a Lck-inhibitory concentration of damnacanthal of 5 mg/kg for the subsequent behavioral experiments (Fig. 4). This concentration had no apparent effects on the levels of the phosphorylated forms of Src and Fyn.

Next, the effect of Lck-inhibition on hippocampus-dependent spatial learning and memory was tested. Damnacanthal was injected i.p. at a dose 5 mg/kg, which did not alter the basic neurological functions, as evaluated by the Irwin [41] observational battery (Table 1), but still led to a significant reduction in Tyr 394 phosphorylation of Lck in the hippocampus (Fig. 4). To exclude a potentially confounding effect of damnacanthal on locomotor and exploratory behaviors, the performance of the damnacanthal-injected mice was evaluated using the open field test. The potential effects of damnacanthal treatment on motor coordination were further evaluated using the Rota Rod. Treatment with 5 mg/kg i.p. damnacanthal ($n = 10$ per group) did not affect either the locomotor or the exploratory activity, as evaluated by the total distance travelled in the open field [$P > 0.05$ (n.s.)] (Fig. 5B), or motor coordination, as measured by the latency to fall off the Rota Rod [$P > 0.05$ (n.s.)] (Fig. 5A).

Mice of both groups were subjected to a learning-acquisition behavioral training in the Morris Water Maze 48 h after the open field test ("Materials and methods"). The damnacanthal-treated mice exhibited significant deficits in the spatial learning task, as evaluated by the latency to reach the hidden platform. The results were averaged over three daily acquisition trials and compared with those of the control animals (Fig. 5C, a–b). Twenty-four hours after the last training trial, a probe trial was conducted in which the time spent in the quadrant that originally contained the platform was used as an indicator of hippocampus-dependent spatial memory. In contrast to the control mice, which displayed a significant preference for the target quadrant, the damnacanthal-treated mice did not spend significantly more time swimming inside the target quadrant than in the remaining three quadrants (Fig. 5D). Collectively, these data indicate that the phosphorylated active forms of Lck play critical roles during both the acquisition and the retention phases of hippocampus-dependent spatial learning and memory.

Discussion

We explored the involvement of the brain protein Lck, a non-receptor tyrosine kinase also known as p56Lck [6], in the regulation of neuronal morphology, memory-related hippocampal synaptic plasticity and in vivo memory acquisition and long-term maintenance. Pharmacological and genetic loss-of-function approaches, which were previously shown to be effective for the inhibition of Lck, were combined here to examine the role of Lck in the mouse hippocampus. The pharmacological experiments were performed using damnacanthal, a selective inhibitor of Lck tyrosine kinase activity [48, 49] that is broadly used as a specific Lck inhibitor in a wide range of cells and tissues [50–54]. We observed using a western blotting analysis that 10 μM damnacanthal inhibited Lck activity in cultured hippocampal neurons. This concentration (10 μM) is significantly lower than those previously reported to inhibit Lck in other cell types [51, 54]. Damnacanthal is over 100 times more selective for Lck than for other serine/threonine kinases (including PKA and PKC), and selectivity for Lck over other members of its kinase-family including Src and Fyn is statistically significant [48, 49]. Differences in the dose-responses and/or in the molecular mechanisms associated with the Lck function might, therefore, vary depending on the cell types, tissues and regions under study or on the preparation types (i.e., primary dissociated cultures vs. sliced brain tissue or in vivo injections, as also reported here) [64]. We also used the Lck inhibitor 4A6H [6, 55] and corroborated the functional involvement of Lck in hippocampal neuritic outgrowth.

Genetically induced hampering of Lck was based on the neuronal transfection of previously characterized specific murine Lck-inhibitory shRNAs that have been reported to be effective for specific Lck silencing [32, 48]. Proof-of-principle qRT-PCR experiments in PC12 cells further demonstrated that this shRNA-based loss-of-function strategy is an effective method for reducing the levels of the Lck protein. The pharmacological and genetic approaches both confirmed the relevance of Lck for neuronal outgrowth, suggesting that Lck might act as regulator of the plasticity-related growth of synaptic structures in the hippocampus during memory formation and maintenance [46].

Neuronal outgrowth is known to be dysregulated in several neuropathologies that affect memory function, some of which could potentially be related to Lck. For instance, exacerbation of Tau phosphorylation results in anomalously sustained Tau-microtubule interactions that contribute to the formation of insoluble Tau aggregates in Alzheimer's disease [65]. Interestingly, Lck, which is a subfamily-B member of the Src-family [3, 4], can phosphorylate several residues of the Tau protein, including

Tyr18 [5]. Fyn, a subfamily-A member of the Src-family [3, 4], has also been proposed to interact with Tau and to be related to the pathogenesis of AD [66, 67]. However, recent experimental evidence indicates that whereas both Lck and Fyn efficiently phosphorylate Tyr18 of Tau, Lck is more effective than Fyn in phosphorylating several other tyrosine residues of Tau [5]. Moreover, moderate levels of Aβ induced an increase in the expression of Fyn, resulting in marked neuronal deficits [14]. In contrast, significantly lower levels of Lck have been observed in the brains of AD patients [19]. These observations therefore suggest the possibility of a differential involvement of Fyn and Lck in the neuronal function and in the molecular mechanisms underlying or mediating Alzheimer's disease. Lck could thus mediate the modulation of the memory-related synaptic function via its demonstrated interaction with the Tau protein, which is not only critical for neuritic outgrowth and axonal development but is further related to Alzheimer's disease, the most prevalent human neuropathology linked to the loss of memory function [5]. More studies are necessary to better understand the physiological significance of Lck as a regulator of neuritic outgrowth and the possible relationship of Lck to neuropathology.

In the current work, we also observed that treatment with the selective Lck-inhibitor damnacanthal had no effect on several primarily AMPAR-related processes (Figs. 2, 3A–C). Glutamate regulates memory formation and maintenance and mediates memory-related synaptic strengthening via the fine-tuned function of both AMPA and NMDA receptors [10, 68–71]. However, the synaptic function can be selectively modulated via NMDAR-mediated synaptic transmission without a need for major changes in the AMPAR-dependent glutamatergic activity [72–76]. Thus, Lck may play a minor role in the regulation of the AMPAR-related presynaptic and postsynaptic mechanisms associated with short-term forms of synaptic strengthening in hippocampal neurons [60–63]. In contrast, our morphological, behavioral, and long-term potentiation experiments suggest that Lck might be specifically involved in the regulation of the long-term forms of memory-related hippocampal synaptic strengthening and in the modulation of neuritic outgrowth, processes that depend profoundly on the activity of *N*-methyl-D-aspartate (NMDA) receptors [46]. Src protein kinase is known to stimulate the activity of the NMDA type of glutamate receptor [8, 77], which has a pivotal role in long-term potentiation (LTP) in the CA1 region of hippocampus. Therefore, our data suggest that Lck can similarly interact with and modulate NMDA receptors, thus playing a causal role in the maintenance of the functional levels of NMDAR-mediated currents that are required for long-term synaptic strengthening, which is also observed for other Src kinase-family members including Src and Fyn [9, 10, 12, 13, 17, 77–79]. Recent studies characterizing the role of other protein kinases in the context of memory-related synaptic plasticity have demonstrated a functional pattern of activity comparable to those presented here for Lck. Kim et al. [80] concluded that both genetic and pharmacological strategies hampering the protein kinase PI3Kγ result in the selective alteration of only a specific form of NMDAR-mediated long-term synaptic plasticity without affecting the basal synaptic properties, including the features of the mEPSCs or paired-pulse induced synaptic strengthening. Additional functional experiments using genetically engineered mice that are deficient in Lck could therefore contribute significantly to the understanding of the role of Lck in hippocampus-mediated memory acquisition and maintenance.

The observation that the inhibition of Lck leads to significantly impaired performance in the Morris Water Maze task further supports the proposed relevance of Lck as a critical regulator of learning and memory. Reduced Lck activity prevented the acquisition of spatial memory because no decrease in the latency to reach the platform over a period of days during training was observed in damnacanthal-treated mice. These data suggest a deficit in long-term memory because the 24-h interval between training days requires the occurrence of protein synthesis-dependent long-term memory processes [81]. Although these results are consistent with a deficit in the long-term LTP resulting from the application of damnacanthal to hippocampal slices, the escape latency could also potentially be affected by nonspecific effects of the drug treatment on swimming performance. This possible confounding factor can, however, be excluded because the damnacanthal treatment did not affect swimming speeds throughout the entire experiment. Additionally, the unaltered motor coordination during the Rota Rod and exploratory activities that was similar to the control levels in the Open Field further rule out any experimental bias due to the application of damnacanthal in the Morris Water Maze. Thus, these data suggest that Lck activity is required for the acquisition of hippocampus-dependent spatial memory and may be explained by the constraints on the synaptic plasticity-related outgrowth induced by Lck-inhibition [33, 81–85].

Thus, this work provides the first comprehensive structural and functional characterization of Lck including its role in the modulation of synaptic plasticity and hippocampus-dependent long-term memory. Our data also invite future experiments investigating a possible differential contribution of Lck relative to other Src kinase family members to the pathogenesis of Alzheimer's disease and other potential uses of Lck as a pharmacological target.

Acknowledgments We thank Ing. Reiner Poldi, the NPI Company and Dr. Gerhard Rammes for expert support during the implementation of the electrophysiological techniques. F.J.M. received financial support from the Hochschul-Jubiläum-Stiftung der Stadt Wien.

References

1. Brugge JS, Erikson RL (1977) Identification of a transformation-specific antigen induced by an avian sarcoma virus. Nature 269:346–348
2. Levinson AD, Oppermann H, Levintow L, Varmus HE, Bishop JM (1978) Evidence that the transforming gene of avian sarcoma virus encodes a protein kinase associated with a phosphoprotein. Cell 15:561–572
3. Benati D, Baldari CT (2008) SRC family kinases as potential therapeutic targets for malignancies and immunological disorders. Curr Med Chem 15:1154–1165
4. Brown MT, Cooper JA (1996) Regulation, substrates and functions of src. Biochim Biophys Acta 1287:121–149
5. Scales TM, Derkinderen P, Leung KY, Byers HL, Ward MA, Price C, Bird IN, Perera T, Kellie S, Williamson R, Anderton BH, Reynolds CH (2011) Tyrosine phosphorylation of tau by the SRC family kinases lck and fyn. Mol Neurodegener 6:12
6. Fenster CP, Chisnell HK, Fry CR, Fenster SD (2010) The role of CD4-dependent signaling in interleukin-16 induced c-Fos expression and facilitation of neurite outgrowth in cerebellar granule neurons. Neurosci Lett 485:212–216
7. Liu G, Beggs H, Jurgensen C, Park HT, Tang H, Gorski J, Jones KR, Reichardt LF, Wu J, Rao Y (2004) Netrin requires focal adhesion kinase and Src family kinases for axon outgrowth and attraction. Nat Neurosci 7:1222–1232
8. Lu YM, Roder JC, Davidow J, Salter MW (1998) Src activation in the induction of long-term potentiation in CA1 hippocampal neurons. Science 279:1363–1367
9. Salter MW (1998) Src, *N*-methyl-D-aspartate (NMDA) receptors, and synaptic plasticity. Biochem Pharmacol 56:789–798
10. Ali DW, Salter MW (2001) NMDA receptor regulation by Src kinase signalling in excitatory synaptic transmission and plasticity. Curr Opin Neurobiol 11:336–342
11. Morita A, Yamashita N, Sasaki Y, Uchida Y, Nakajima O, Nakamura F, Yagi T, Taniguchi M, Usui H, Katoh-Semba R, Takei K, Goshima Y (2006) Regulation of dendritic branching and spine maturation by semaphorin3A-Fyn signaling. J Neurosci 26:2971–2980
12. Grant SG, O'Dell TJ, Karl KA, Stein PL, Soriano P, Kandel ER (1992) Impaired long-term potentiation, spatial learning, and hippocampal development in fyn mutant mice. Science 258: 1903–1910
13. Miyakawa T, Yagi T, Kitazawa H, Yasuda M, Kawai N, Tsuboi K, Niki H (1997) Fyn-kinase as a determinant of ethanol sensitivity: relation to NMDA-receptor function. Science 278:698–701
14. Chin J, Palop JJ, Puolivali J, Massaro C, Bien-Ly N, Gerstein H, Scearce-Levie K, Masliah E, Mucke L (2005) Fyn kinase induces synaptic and cognitive impairments in a transgenic mouse model of Alzheimer's disease. J Neurosci 25:9694–9703
15. Hunter T (1987) A thousand and one protein kinases. Cell 50: 823–829
16. Cotton PC, Brugge JS (1983) Neural tissues express high levels of the cellular src gene product pp 60c-src. Mol Cell Biol 3:1157–1162
17. Umemori H, Ogura H, Tozawa N, Mikoshiba K, Nishizumi H, Yamamoto T (2003) Impairment of *N*-methyl-D-aspartate receptor-controlled motor activity in LYN-deficient mice. Neuroscience 118:709–713
18. Sudol M, Hanafusa H (1986) Cellular proteins homologous to the viral yes gene product. Mol Cell Biol 6:2839–2846
19. Hata R, Masumura M, Akatsu H, Li F, Fujita H, Nagai Y, Yamamoto T, Okada H, Kosaka K, Sakanaka M, Sawada T (2001) Up-regulation of calcineurin Abeta mRNA in the Alzheimer's disease brain: assessment by cDNA microarray. Biochem Biophys Res Commun 284:310–316
20. Blacker D, Bertram L, Saunders AJ, Moscarillo TJ, Albert MS, Wiener H, Perry RT, Collins JS, Harrell LE, Go RC, Mahoney A, Beaty T, Fallin MD, Avramopoulos D, Chase GA, Folstein MF, McInnis MG, Bassett SS, Doheny KJ, Pugh EW, Tanzi RE (2003) Results of a high-resolution genome screen of 437 Alzheimer's disease families. Hum Mol Genet 12:23–32
21. Zhong W, Yamagata HD, Taguchi K, Akatsu H, Kamino K, Yamamoto T, Kosaka K, Takeda M, Kondo I, Miki T (2005) Lymphocyte-specific protein tyrosine kinase is a novel risk gene for Alzheimer disease. J Neurol Sci 238:53–57
22. Omri B, Crisanti P, Marty MC, Alliot F, Fagard R, Molina T, Pessac B (1996) The Lck tyrosine kinase is expressed in brain neurons. J Neurochem 67:1360–1364
23. Glaichenhaus N, Shastri N, Littman DR, Turner JM (1991) Requirement for association of p56lck with CD4 in antigen-specific signal transduction in T cells. Cell 64:511–520
24. Veillette A, Davidson D (1992) Src-related protein tyrosine kinases and T-cell receptor signalling. Trends Genet 8:61–66
25. Mustelin T, Burn P (1993) Regulation of src family tyrosine kinases in lymphocytes. Trends Biochem Sci 18:215–220
26. Nunez J (2008) Primary culture of hippocampal neurons from P0 newborn rats. J Vis Exp 19:895
27. Zeitelhofer M, Vessey JP, Xie Y, Tubing F, Thomas S, Kiebler M, Dahm R (2007) High-efficiency transfection of mammalian neurons via nucleofection. Nat Protoc 2:1692–1704
28. Mosmann T (1983) Rapid colorimetric assay for cellular growth and survival: application to proliferation and cytotoxicity assays. J Immunol Methods 65:55–63
29. Kawabe H, Neeb A, Dimova K, Young SM Jr, Takeda M, Katsurabayashi S, Mitkovski M, Malakhova OA, Zhang DE, Umikawa M, Kariya K, Goebbels S, Nave KA, Rosenmund C, Jahn O, Rhee J, Brose N (2010) Regulation of Rap2A by the ubiquitin ligase Nedd4-1 controls neurite development. Neuron 65:358–372
30. Shirasu M, Kimura K, Kataoka M, Takahashi M, Okajima S, Kawaguchi S, Hirasawa Y, Ide C, Mizoguchi A (2000) VAMP-2 promotes neurite elongation and SNAP-25A increases neurite sprouting in PC12 cells. Neurosci Res 37:265–275
31. Slimko EM, McKinney S, Anderson DJ, Davidson N, Lester HA (2002) Selective electrical silencing of mammalian neurons in vitro by the use of invertebrate ligand-gated chloride channels. J Neurosci 22:7373–7379
32. Fan G, Simmons MJ, Ge S, Dutta-Simmons J, Kucharczak J, Ron Y, Weissmann D, Chen CC, Mukherjee C, White E, Gelinas C (2010) Defective ubiquitin-mediated degradation of antiapoptotic Bfl-1 predisposes to lymphoma. Blood 115:3559–3569
33. Monje FJ, Kim EJ, Pollak DD, Cabatic M, Li L, Baston A, Lubec G (2011) Focal adhesion kinase regulates neuronal growth, synaptic plasticity and hippocampus-dependent spatial learning and memory. Neurosignals 20:1–14
34. Casey SC, Nelson EL, Turco GM, Janes MR, Fruman DA, Blumberg B (2011) B-1 cell lymphoma in mice lacking the steroid and xenobiotic receptor, SXR. Mol Endocrinol 25:933–943
35. Levine A, Huang Y, Drisaldi B, Griffin EA Jr, Pollak DD, Xu S, Yin D, Schaffran C, Kandel DB, Kandel ER (2011) Molecular mechanism for a gateway drug: epigenetic changes initiated by nicotine prime gene expression by cocaine. Sci Transl Med 3:107ra109

36. Simon W, Hapfelmeier G, Kochs E, Zieglgansberger W, Rammes G (2001) Isoflurane blocks synaptic plasticity in the mouse hippocampus. Anesthesiology 94:1058–1065
37. Rammes G, Starker LK, Haseneder R, Berkmann J, Plack A, Zieglgansberger W, Ohl F, Kochs EF, Blobner M (2009) Isoflurane anaesthesia reversibly improves cognitive function and long-term potentiation (LTP) via an up-regulation in NMDA receptor 2B subunit expression. Neuropharmacology 56:626–636
38. Nguyen PV, Kandel ER (1997) Brief theta-burst stimulation induces a transcription-dependent late phase of LTP requiring cAMP in area CA1 of the mouse hippocampus. Learn Mem 4: 230–243
39. Malleret G, Alarcon JM, Martel G, Takizawa S, Vronskaya S, Yin D, Chen IZ, Kandel ER, Shumyatsky GP (2010) Bidirectional regulation of hippocampal long-term synaptic plasticity and its influence on opposing forms of memory. J Neurosci 30:3813–3825
40. Huang YY, Kandel ER (1994) Recruitment of long-lasting and protein kinase A-dependent long-term potentiation in the CA1 region of hippocampus requires repeated tetanization. Learn Mem 1:74–82
41. Irwin S (1968) Comprehensive observational assessment: Ia. A systematic, quantitative procedure for assessing the behavioral and physiologic state of the mouse. Psychopharmacologia 13:222–257
42. Pollak D, Weitzdoerfer R, Yang YW, Prast H, Hoeger H, Lubec G (2005) Cerebellar protein expression in three different mouse strains and their relevance for motor performance. Neurochem Int 46:19–29
43. Pollak DD, Scharl T, Leisch F, Herkner K, Villar SR, Hoeger H, Lubec G (2005) Strain-dependent regulation of plasticity-related proteins in the mouse hippocampus. Behav Brain Res 165: 240–246
44. Rouer E (2010) Neuronal isoforms of Src, Fyn and Lck tyrosine kinases: A specific role for p56lckN in neuron protection. CR Biol 333:1–10
45. Zamoyska R, Basson A, Filby A, Legname G, Lovatt M, Seddon B (2003) The influence of the src-family kinases, Lck and Fyn, on T cell differentiation, survival and activation. Immunol Rev 191:107–118
46. Kandel ER (2001) The molecular biology of memory storage: a dialogue between genes and synapses. Science 294:1030–1038
47. Kandel ER, Schwartz JH (1982) Molecular biology of learning: modulation of transmitter release. Science 218:433–443
48. Faltynek CR, Schroeder J, Mauvais P, Miller D, Wang S, Murphy D, Lehr R, Kelley M, Maycock A, Michne W et al (1995) Damnacanthal is a highly potent, selective inhibitor of p56lck tyrosine kinase activity. Biochemistry 34:12404–12410
49. Faltynek CR, Wang S, Miller D, Mauvais P, Gauvin B, Reid J, Xie W, Hoekstra S, Juniewicz P, Sarup J et al (1995) Inhibition of T lymphocyte activation by a novel p56lck tyrosine kinase inhibitor. J Enzyme Inhib 9:111–122
50. Toth A, Szilagyi O, Krasznai Z, Panyi G, Hajdu P (2009) Functional consequences of Kv1.3 ion channel rearrangement into the immunological synapse. Immunol Lett 125:15–21
51. Phillippe M, Sweet LM, Bradley DF, Engle D (2009) Role of nonreceptor protein tyrosine kinases during phospholipase C-gamma 1-related uterine contractions in the rat. Reprod Sci 16:265–273
52. Inngjerdingen M, Torgersen KM, Maghazachi AA (2002) Lck is required for stromal cell-derived factor 1 alpha (CXCL12)-induced lymphoid cell chemotaxis. Blood 99:4318–4325
53. Yao Z, Zhang J, Dai J, Keller ET (2001) Ethanol activates NFkappaB DNA binding and p56lck protein tyrosine kinase in human osteoblast-like cells. Bone 28:167–173
54. Aoki K, Parent A, Zhang J (2000) Mechanism of damnacanthal-induced [Ca(2 +)](i) elevation in human dermal fibroblasts. Eur J Pharmacol 387:119–124
55. Von Knethen A, Abts H, Kube D, Diehl V, Tesch H (1997) Expression of p56lck in B-cell neoplasias. Leuk Lymphoma 26:551–562
56. Wu Y, Sheng W, Chen L, Dong H, Lee V, Lu F, Wong CS, Lu WY, Yang BB (2004) Versican V1 isoform induces neuronal differentiation and promotes neurite outgrowth. Mol Biol Cell 15:2093–2104
57. Arthur DB, Akassoglou K, Insel PA (2006) P2Y2 and TrkA receptors interact with Src family kinase for neuronal differentiation. Biochem Biophys Res Commun 347:678–682
58. Theus MH, Wei L, Francis K, Yu SP (2006) Critical roles of Src family tyrosine kinases in excitatory neuronal differentiation of cultured embryonic stem cells. Exp Cell Res 312:3096–3107
59. Creager R, Dunwiddie T, Lynch G (1980) Paired-pulse and frequency facilitation in the CA1 region of the in vitro rat hippocampus. J Physiol 299:409–424
60. Del Castillo J, Katz B (1954) Statistical factors involved in neuromuscular facilitation and depression. J Physiol 124:574–585
61. Kuhnt U, Voronin LL (1994) Interaction between paired-pulse facilitation and long-term potentiation in area CA1 of guinea-pig hippocampal slices: application of quantal analysis. Neuroscience 62:391–397
62. Voronin LL (1994) Quantal analysis of hippocampal long-term potentiation. Rev Neurosci 5:141–170
63. Zucker RS, Regehr WG (2002) Short-term synaptic plasticity. Annu Rev Physiol 64:355–405
64. Szczot M, Wojtowicz T, Mozrzymas JW (2010) GABAergic and glutamatergic currents in hippocampal slices and neuronal cultures show profound differences: a clue to a potent homeostatic modulation. J Physiol Pharmacol 61:501–506
65. Cohen TJ, Guo JL, Hurtado DE, Kwong LK, Mills IP, Trojanowski JQ, Lee VM (2011) The acetylation of tau inhibits its function and promotes pathological tau aggregation. Nat Commun 2:252
66. Lee G, Newman ST, Gard DL, Band H, Panchamoorthy G (1998) Tau interacts with src-family non-receptor tyrosine kinases. J Cell Sci 111(Pt 21):3167–3177
67. Bhaskar K, Yen SH, Lee G (2005) Disease-related modifications in tau affect the interaction between Fyn and Tau. J Biol Chem 280:35119–35125
68. Mattson MP (2008) Glutamate and neurotrophic factors in neuronal plasticity and disease. Ann NY Acad Sci 1144:97–112
69. MacDonald JF, Jackson MF, Beazely MA (2006) Hippocampal long-term synaptic plasticity and signal amplification of NMDA receptors. Crit Rev Neurobiol 18:71–84
70. Tsien JZ, Huerta PT, Tonegawa S (1996) The essential role of hippocampal CA1 NMDA receptor-dependent synaptic plasticity in spatial memory. Cell 87:1327–1338
71. Tonegawa S, Tsien JZ, McHugh TJ, Huerta P, Blum KI, Wilson MA (1996) Hippocampal CA1-region-restricted knockout of NMDAR1 gene disrupts synaptic plasticity, place fields, and spatial learning. Cold Spring Harb Symp Quant Biol 61:225–238
72. Campioni MR, Xu M, McGehee DS (2009) Stress-induced changes in nucleus accumbens glutamate synaptic plasticity. J Neurophysiol 101:3192–3198
73. Kim J, Jung SY, Lee YK, Park S, Choi JS, Lee CJ, Kim HS, Choi YB, Scheiffele P, Bailey CH, Kandel ER, Kim JH (2008) Neuroligin-1 is required for normal expression of LTP and associative fear memory in the amygdala of adult animals. Proc Natl Acad Sci USA 105:9087–9092
74. Nakayama K, Kiyosue K, Taguchi T (2005) Diminished neuronal activity increases neuron–neuron connectivity underlying silent

synapse formation and the rapid conversion of silent to functional synapses. J Neurosci 25:4040–4051
75. Van Sickle BJ, Xiang K, Tietz EI (2004) Transient plasticity of hippocampal CA1 neuron glutamate receptors contributes to benzodiazepine withdrawal-anxiety. Neuropsychopharmacology 29:1994–2006
76. Wyllie DJ, Manabe T, Nicoll RA (1994) A rise in postsynaptic Ca^{2+} potentiates miniature excitatory postsynaptic currents and AMPA responses in hippocampal neurons. Neuron 12:127–138
77. Yu XM, Askalan R, Keil GJ 2nd, Salter MW (1997) NMDA channel regulation by channel-associated protein tyrosine kinase Src. Science 275:674–678
78. Hayashi T, Umemori H, Mishina M, Yamamoto T (1999) The AMPA receptor interacts with and signals through the protein tyrosine kinase Lyn. Nature 397:72–76
79. Yaka R, Phamluong K, Ron D (2003) Scaffolding of Fyn kinase to the NMDA receptor determines brain region sensitivity to ethanol. J Neurosci 23:3623–3632
80. Kim JI, Lee HR, Sim SE, Baek J, Yu NK, Choi JH, Ko HG, Lee YS, Park SW, Kwak C, Ahn SJ, Choi SY, Kim H, Kim KH, Backx PH, Bradley CA, Kim E, Jang DJ, Lee K, Kim SJ, Zhuo M, Collingridge GL, Kaang BK (2011) PI3Kgamma is required for NMDA receptor-dependent long-term depression and behavioral flexibility. Nat Neurosci 14:1447–1454
81. Bekinschtein P, Cammarota M, Igaz LM, Bevilaqua LR, Izquierdo I, Medina JH (2007) Persistence of long-term memory storage requires a late protein synthesis- and BDNF-dependent phase in the hippocampus. Neuron 53:261–277
82. Patterson SL, Abel T, Deuel TA, Martin KC, Rose JC, Kandel ER (1996) Recombinant BDNF rescues deficits in basal synaptic transmission and hippocampal LTP in BDNF knockout mice. Neuron 16:1137–1145
83. Conner JM, Franks KM, Titterness AK, Russell K, Merrill DA, Christie BR, Sejnowski TJ, Tuszynski MH (2009) NGF is essential for hippocampal plasticity and learning. J Neurosci 29:10883–10889
84. Xu B, Gottschalk W, Chow A, Wilson RI, Schnell E, Zang K, Wang D, Nicoll RA, Lu B, Reichardt LF (2000) The role of brain-derived neurotrophic factor receptors in the mature hippocampus: modulation of long-term potentiation through a presynaptic mechanism involving TrkB. J Neurosci 20:6888–6897
85. Monje FJ, Kassabov S, Fiumara F, Bailey CH, Kandel ER (2008) A novel leucine-rich-repeat tyrosine-kinase promotes growth factor signaling, neuritic outgrowth and long-term facilitation in aplysia. FENS Abstr 4(079):15